

Initial Access Codebook Design and CSI Type-II Feedback for Sub-6GHz 5G NR

Ryan M. Dreifuerst, *Student Member, IEEE*, and Robert W. Heath Jr. *Fellow, IEEE*

Abstract

Beam codebooks are a recent feature to enable high dimension multiple-input multiple-output (MIMO) in 5G new radio (NR). Codebooks comprised of customizable beamforming weights can be used to transmit reference signals and aid the channel state information (CSI) acquisition process. In this paper, we characterize the role of each codebook used during the beam management process and design a neural network to find codebooks that improve overall system performance. Evaluating a codebook is not purely about maximizing signal power, but instead, a holistic, system-level view of effective spectral efficiency is necessary to capture the relationships between codebooks, feedback, and spectral efficiency. The proposed algorithm is built on translating codebook and feedback knowledge into a consistent beamspace basis similar to a virtual channel model to generate initial access codebooks and select the subsequent refined beam training. This beamspace codebook algorithm is designed to directly integrate with current 5G beam management standards. Simulation results show that the neural network codebooks improve over traditional codebooks in received signal power, even in dispersive sub-6GHz environments. We further utilize our simulation framework to evaluate type-II CSI feedback formats with regard to effective multi-user spectral efficiency. Our results suggest that optimizing codebook performance can provide valuable spectral efficiency improvements, but 5G feedback quantization resolution limits multi-user performance in sub-6GHz bands due to the rich scattering environment.

I. INTRODUCTION

Fifth-generation (5G) cellular systems have adopted a beam-based approach for MIMO communications. In such systems, broadcast control signals are beamformed in a specific direction to provide array gain [1]. This helps overcome challenging propagation environments with adaptive

Ryan M. Dreifuerst and Robert W. Heath Jr. are with North Carolina State University, Raleigh, NC 27695 {rmdreifu, rwheathjr}@ncsu.edu. This work was supported in part by NSF Grant No. NSF-CCF-2225555 and NSF-CNS-2147955.

array beamforming in 5G. While the motivation for beam-based systems was to aid millimeter-wave (mmWave) frequency bands, the same framework is also used at low frequencies. Unfortunately, optimization of the beamforming framework, and subsequent feedback strategies, has not been extensively developed for sub-6GHz MIMO, despite its continued importance in standards.

Codebook-based beam management is a framework for beamforming and feedback that enables transmitting beamformed reference signals and multiple forms of CSI acquisition [1]. In early 3GPP releases up to Release 12, channel state information (CSI) was obtained by estimating the channel from reference signals for every transmitter-receiver beam pair using unprecoded signals. The use of unprecoded reference signals was used up through 4G LTE Release 14 because multi-antenna beamforming was not needed to achieve higher signal-to-noise ratio (SNR) for synchronization and channel estimation. Beamformed control signals have become a necessity in mmWave bands as a result of the increasing bandwidths (which reduce the SNR for a constant transmit power), increasing NLOS path loss, and shrinking antennas sizes—resulting in pre-beamformed SNR on the order of -15dB or less [2]. By beamforming the control and reference signals, receivers are more likely to detect initial access signals and obtain more accurate synchronization and channel measurements.

The process of obtaining CSI at the transmitter is a challenge for large antenna arrays due to the increasing overhead and feedback for pilot-based estimation. 5G NR uses a beam management protocol to train analog arrays with minimal feedback in the form of codebook indices corresponding to training beams received. By including both a beam training and channel estimation phase in the standards, the arrays can be configured in a hybrid format where one logical port can be fed to an analog subarray. This allows for larger arrays that apply a frequency flat precoding or combining without needing to explicitly estimate the channel for each of these antennas. Instead, only the digital dimension (or ports in 5G terminology) is estimated. Upon completing beam training and channel measurement, the user equipment prepares a packet of information to feedback to the base station. The feedback is determined based on a CSI codebook (i.e. type-I or type-II) that facilitates quantizing the information.

In addition to the type-I and type-II CSI feedback codebooks, there are two more codebooks that are associated with the initial access and beam refinement stages [3], [4]. These codebooks play three roles in the 5G framework that are often merged or misunderstood in literature. First,

wide-beam codebooks are used to regularly transmit synchronization signal blocks (SSB) and begin initial access. Second, narrow-beam codebooks are used to transmit CSI reference signals (CSI-RS) which enable high SNR channel estimation and precise analog beam training. The codebooks corresponding to the SSB and CSI-RS signals facilitate a hierarchical beam search [5], although there is no requirement that the SSB beamformers be “wide” nor that the CSI-RS beamformers be “narrow” in angular space. Due to multipath propagation, it is possible that the best codebooks are not simply wide and narrow. Finally, a third, standardized codebook which is used to generate the quantized CSI feedback from user equipment (UE) to base stations (BS). Of all of the codebooks, only the codebook used for feedback quantization is defined (depending on the BS logical array geometry) because it must be understood by both the UE(s) and BS. In contrast, the UE does not need to know the SSB or CSI-RS beamforming codewords/vectors used. It is not strictly necessary that even the feedback codebook is known when reciprocity exists, as typically seen in time-division-duplexing systems. It is generally the case that even in these systems, feedback from downlink training is still beneficial due to asynchronous link budgets [6] or when the number of transmitting and receiving antennas on a UE is not equal [7].

Our contributions in this manuscript are as follows:

- First, we precisely describe the beam management and CSI type-II feedback approach for 5G networks. There are many misconceptions on how the codebooks, SSB, and CSI-RS processes are used for obtaining various forms of feedback. We explain how the various codebooks are used, what is specified in the standards versus left up to implementations, and provide an efficient implementation for feedback quantization in CSI type-II.
- We present a novel neural network architecture, Beamspace-Codex (BSC), and feedback processing technique for SSB codebook generation. We explicitly constrain the system to follow 5G beam management time constraints which presents a significant constraint for translating the SSB feedback for CSI-RS codebook generation. To manage this constraint, the SSB codebook is dynamically generated—which is manageable at the SSB periodicity—and the CSI-RS codebook is determined as a precomputed DFT decomposition of the SSB codebook. With this integration, we unify the arbitrary codebooks learned via deep learning with the feedback quantization technique to facilitate a hierarchical beam search that improves the beam management process used in 5G NR.

- Finally, we present the results of an extensive evaluation of our proposed method with standard DFT codebooks and CSI-based eigen-beamforming solutions using various levels of feedback and overhead. We show that our proposed solution achieves significant performance improvements. We also show that MU-MIMO performance is dramatically limited by the quantization resolution techniques in low-band 5G. In contrast, the frequency selectivity and resource allocation have little impact in the current framework and scattering environment.

There is significant work on beam training and beam alignment, however, herein we review a set of relevant prior work relating to machine learning and beam training. In [8], a gradient-optimization approach, not using deep learning, is shown to be successful in aiding the beam search process with respect to maximizing the SNR in 60GHz personal networks. Another approach using classical data-driven techniques is presented in [9] for vehicular networks based on historical beam training results. While the codebooks and algorithms are relatively straightforward, the idea of “learning” an efficient codebook from site-specific data is a cornerstone of many modern beam alignment techniques [10]–[13]. These papers all focus on mmWave channels and often exploit the sparsity of such environments to aid the beam training process. Furthermore, all of these papers focus exclusively on beam alignment using DFT codebooks. While DFT codebooks are especially effective in limited scattering environments at mmWave bands, these codebooks do not necessarily work well in rich scattering environments. Furthermore, none of these papers consider a MIMO format with more than one antenna for each UE, even though maintaining a link in mmWave bands essentially necessitates user-side beamforming. In this paper we consider a full MU-MIMO OFDM system in a rich scattering environment and utilize dynamic and arbitrary codebooks.

In another line of related work, algorithms have been proposed that design beamformers or codebooks [12], [14]–[18]. Hierarchical codebooks were proposed in [14] which separated the beam training into multiples stages of wide-beam and narrow-beam codebooks. A similar strategy was adopted by 5G using the SSB and CSI-RS codebooks and plays an important role in systems designed for 5G deployment. Deep learning was applied to the task in [15], which uses deep reinforcement learning to design broadcast beam patterns. While designed for small-scale MIMO, the results suggest that arbitrary learned beam patterns can be an effective way to initiate

communication in broadband networks. A supervised and an unsupervised learning approach were presented in [16], which showed nearly optimal results when used to design beamforming vectors from channel measurements. These results were based on a highly simplified channel model though, and perfect CSI was assumed at the BS. Recently, a deep, federated, reinforcement learning strategy was proposed [12] that jointly trained a beam management model over a network using user location information. The focus was on deciding which sectors would be active, thereby narrowing the “codebook”, although the paper ignores all beamforming besides sector-level association and large-scale pathloss. Another paper considered a situation for learning probing beams [17], which is one of the only papers to consider both the SSB and CSI-RS codebooks. The results show significant gains can be achieved over a basic hierarchical search, although perfect CSI is assumed to be available for training and the channels are assumed to be narrowband. [17] provides motivation for researching realistic deep learning codebook methods. In our previous work [18] we designed a neural network for SSB codebook generation in narrowband channels as well, but trained using an angular representation of the channel. The results, however, did not extend well to wideband systems and did not consider the impact that the SSB codebook has on system-level performance. In this investigation, we now model wideband channels and fully incorporate the entire beam management and data transmission into our evaluation.

The third focus of our research is on the relationship between beam management and the feedback framework used in 5G networks. An enhanced CSI feedback strategy was proposed for full-dimension MIMO [19] in 4G Release 13 which is based on a linear combination of DFT codewords. This strategy is very similar to the type-II feedback format introduced in 5G Release 15. One key difference is that the proposal assumed the users must know the beamforming vector used during pilot transmission, which was not adopted into the standards. There has also been growing interest in utilizing machine learning for feedback [20]–[22]. These works assume that both the network and the users can share models for encoding and decoding the feedback, which is not supported or easily introduced into network operation. In this paper we do not use deep learning to change the feedback methods, but instead, look at the relationship and limitations the feedback and beam management strategy have on MU-MIMO performance.

The remainder of our paper is organized as follows. First, we provide background on beam management operation for 5G NR. Then, we introduce the system model beginning from a multi-

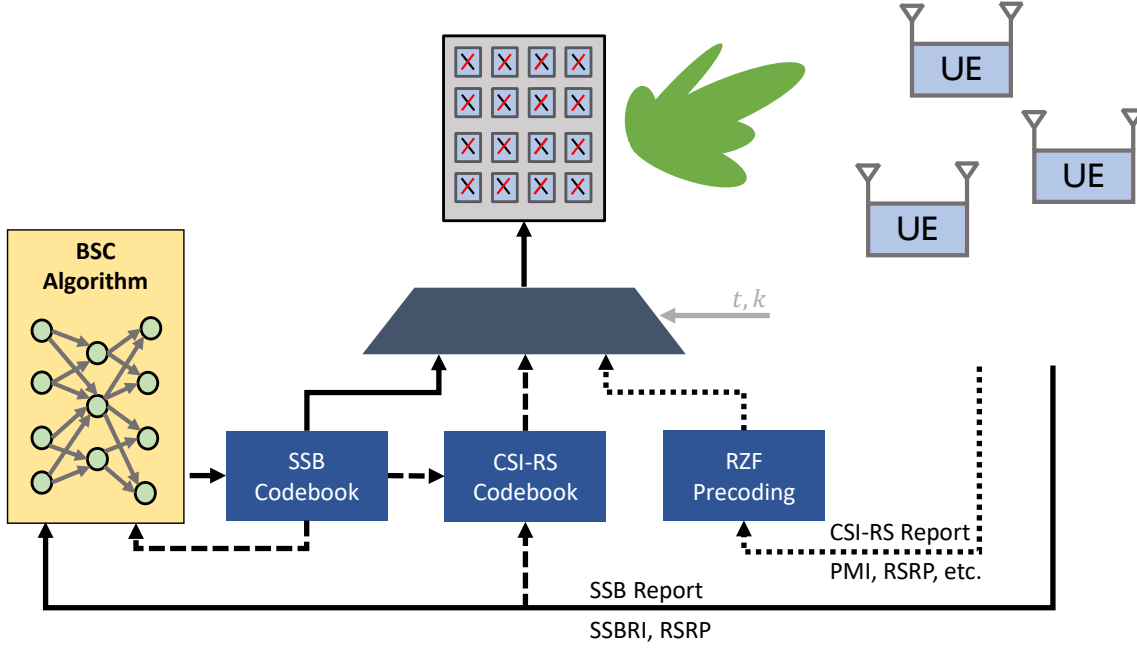


Fig. 1. Beamforming codebooks are used to transmit reference signals for synchronization from the SSB codebook. Based on the SSB report, additional reference signals are beamformed using the CSI-RS codebook for channel estimation by the user equipment (UEs). Using the CSI-RS report, the base station can design a precoder (i.e. RZF precoder) that attempts to maximize the spectral efficiency. The proposed BSC algorithm updates the SSB codebook, which in turn affects the CSI-RS codebook and feedback.

path channel model and continuing up through the two metrics of interest: RSRP and spectral efficiency (SE). Next, we introduce the beamspace observation and neural network architecture that form the basis of our work. In the final sections, we present the simulation setup and evaluate the various codebooks and feedback formats to address the lack of prior work when it comes to codebooks and CSI formats in sub-6GHz 5G NR.

Notation: \mathbf{A} is a matrix, \mathbf{a} and $\{a[i]\}_{i=1}^N$ are column vectors and a, A denote scalars. \mathbf{A}^T , $\overline{\mathbf{A}}$, \mathbf{A}^* , and \mathbf{A}^\dagger represent the transpose, conjugate, conjugate transpose, and psuedo-inverse of \mathbf{A} . The real and imaginary parts of \mathbf{A} are denoted by $\mathbb{R}(\mathbf{A})$ and $\mathbb{I}(\mathbf{A})$. $\mathbf{A}[k, \ell]$ denotes the entry of \mathbf{A} in the k^{th} row and the ℓ^{th} column. The same meaning is also associated with $\mathbf{A}_{k, \ell}$. a_ℓ refers to the ℓ^{th} element of \mathbf{a} and \mathbf{a}_ℓ refers to the ℓ^{th} column of \mathbf{A} . Similarly, $\mathbf{A}[:, k]$ refers to the k^{th} column of \mathbf{A} . Unspecified norm equations are $\|\mathbf{a}\|_2 = \mathbf{a}^* \mathbf{a}$ for vectors and the Frobenius norm $\|\mathbf{A}\|_F = \sqrt{\text{Tr}(\mathbf{A} \mathbf{A}^*)}$ for matrices. We make use of the disjoint operator $\mathbf{A} \setminus \alpha$ to describe the matrix (or vector) \mathbf{A} excluding the subset (or element) α . We define $j = \sqrt{-1}$. Due to the notational complexity of MU-MIMO with OFDM, we will always use u to refer to a specific UE, t as a specific time, k as a specific frequency resource, and n_t / n_r to refer to a specific transmit

or receive antenna. OFDM channels will be italicized like \mathbf{H} while time-domain channels are written as H .

II. BACKGROUND

We first provide a brief background on the specifications and steps (according to Release 16) involved in initial access and beam refinement in 5G NR. We describe the task from a sub-6GHz cell perspective. The base station cell routinely transmits SSBs with different beamforming vectors and the UE provides a short packet of feedback containing only basic channel and beam selection properties. The BS will use the reported SSB information to select precise beamforming vectors to use for CSI-RS transmission. We use this information to motivate a system model that integrates codebook-based beamforming and feedback. Using this model, we evaluate the beam-based system based on network metrics such as spectral efficiency.

Initial access is used in mobile networks to obtain very limited channel information, achieve synchronization, and set up random access procedures. In 5G NR, a cell may initiate the initial access period at regular intervals of $\{5, 10, 20, 40, 80, 160\}$ ms [4], to control the periodicity a UE must be active and provide feedback to the network. During this period, the cell will transmit SSBs that contain primary and secondary synchronization signals (PSS, SSS) as well as demodulation reference signals (DMRS) [4]. These SSBs are beamformed using a specific beamforming vector selected from a codebook and associated with a beam index. Each SSB is transmitted iteratively in time, using 20 contiguous resource blocks. This is a much smaller bandwidth than the downlink data transmission and is a key limitation of relying on SSB feedback in frequency-selective channels. Furthermore, the resource allocation of SSB is essentially fixed to assist new users with joining a network. Depending on the cell carrier frequency and subcarrier spacing a cell may transmit up to $L_{\max} = \{1, 4, 8, 64\}$ beams in a burst, and all cells must transmit at least one beam. During transmission, the UE will measure the Reference Signal Received Power (RSRP) and report the measurement using the random access channel slot corresponding to the index of the beam with the highest RSRP. This way the base station knows how strong the signal was and which of the codewords it corresponds to.

Beam refinement is the second step of the hierarchical beam management process that is used to obtain better beam alignment and enable wideband channel estimation. In contrast to SSB signals, CSI-RS are extremely flexible with many combinations of time and frequency resources

allocatable. There are some limitations on how often CSI-RS can be transmitted, but the default periodicity a UE expects when joining the network is 80ms and the symbols should span a larger bandwidth than the SSB—at least 24 resource blocks and up to the entire bandwidth should contain CSI-RS symbols for a measurement report. Furthermore, CSI-RS are also transmitted both periodically and aperiodically to assist beam tracking with highly mobile users. All told, the beam refinement stage requires more resources than initial access, which is why a hierarchical beam search is used to limit the number of CSI-RS processes needed to achieve a strong connection.

PMI feedback is not a strictly required element within a CSI measurement report, but rather configured to achieve a balance of information and overhead. At first glance, this allows for reciprocity-based systems to not waste overhead with PMI feedback, which can span hundreds of bits. In the uplink control channel, the spectral efficiency is often low, i.e. the default max code rate is 0.8bps/Hz [23], and uplink resources are limited so reducing feedback is a critical concern. The reduction of PMI is not only useful with reciprocity, however, it can also enable fast and efficient rank-one beamforming. By only providing the best-beam index the amount of feedback is reduced and a modest beamforming candidate is known. We will consider this method, along with the associated reduced overhead, in our simulation comparisons in Section VI.

III. SYSTEM MODEL

We begin our investigation with an overview of the multipath analytical channel model and SSB beamforming used in initial access and downlink data transmission. Afterward, we define the metrics of interest for our framework and problem formulation. Throughout this paper, we will limit the problem to a single cell with multiple UEs each equipped with multiple antennas and all arrays are fully digital and single-polarization. While the inclusion of multiple cells is more realistic, the impact of multi-cell interference on beam management and feedback is not significant and can be mitigated with limited coordination between nearby cells. The use of single-polarized arrays is a significant assumption in rich scattering environments, but, it is always possible to operate a dual-polarized array as a repetition of single polarization. We will investigate multiple BS deployments with dual-polarized arrays in future work.

A. *MU-MIMO channel model*

We model the system so that it is representative of real-world conditions to analyze a realistic beam training scenario for sub-6GHz M-MIMO. We do not explicitly specify TDD or FDD

because our work does not rely on channel reciprocity. We assume a half-wavelength spaced uniform planar array (UPA) with $N_X \times N_Y$ elements at the base station in a downlink broadcast transmission. The steering vectors $\mathbf{A}(\theta, \phi) \in \mathbb{C}^{N_X \times N_Y}$ are the Kronecker product of the steering vectors of a uniform linear array (ULA) in each dimension $\mathbf{a}(\theta, \phi) = \mathbf{a}(\theta) \otimes \mathbf{a}(\phi)$. The responses are given by the Vandermonde vector and Kronecker product

$$\mathbf{a}_N(\theta) = [1, e^{j\pi \cos \theta}, e^{j2\pi \cos \theta}, \dots, e^{j(N-1)\pi \cos \theta}]^T \quad (1)$$

$$\mathbf{A}(\theta, \phi) = \mathbf{a}_{N_X}(\theta) \otimes \mathbf{a}_{N_Y}(\phi) \in \mathbb{C}^{N_X \times N_Y}. \quad (2)$$

We further assume that the channel is constant over a resource block and that timing and frame synchronization have already been obtained through the PSS and SSS parts of the SSB. The channel is defined for the angular pairs between receiver u and the transmitter, $(\theta_\ell^{(u)}, \phi_\ell^{(u)}), (\theta_\ell^T, \phi_\ell^T)$ and complex path gain α_ℓ for a set of L_p paths with corresponding delays τ_ℓ and filtering/pulse shaping $p(t)$ as

$$\mathcal{H}^{(u)}[\ell] = \alpha_\ell \mathbf{A}(\theta_\ell^{(u)}, \phi_\ell^{(u)}) \otimes \mathbf{A}^*(\theta_\ell^T, \phi_\ell^T) p(\ell\tau - \tau_\ell) \quad (3)$$

$$\in \mathbb{C}^{(N_X^R \times N_Y^R) \times (N_X^T \times N_Y^T)}. \quad (4)$$

The same result as (3) can be achieved by viewing the channel as the tensor product of the two-dimensional azimuth channel response and elevation channel response for each path. Note that the system is not narrowband due to the significant difference in delays between paths relative to 5G sampling rates. We further restrict the system to only consider a ULA at the receiver, equivalent to setting $N_X^R = 1$, and simplifying the channel tap's components to a three-dimensional tensor. It is typical that modern UEs are equipped with ULA, rather than UPA, but the subsequent steps are essentially identical regardless of the user antenna geometry. The UE's array is assumed to be oriented toward the base station, although the UE does not necessarily have a LOS channel. In many future steps, it will be useful to stack the channel as a 2D response of the $N_T = N_X N_Y$ such that

$$\mathbf{H}_{i,k}^{(u)}[\ell] = \mathcal{H}_{i,n,m}^{(u)}[\ell] \quad \forall i \in \{0, 1, \dots, N_R\}, k = nN_X + m. \quad (5)$$

This representation allows for approaching planar arrays with traditional MIMO techniques [24].

We further extend the system model to utilize orthogonal frequency division multiplexing (OFDM)

as a means of handling the frequency selective, wideband channel. In particular, we consider the frequency response of the channels effectively obtained through a K -point inverse discrete Fourier transform (IDFT) at the transmitter and discrete Fourier transform (DFT) at the receiver with zero padding/insertion. The channel response forms a time-frequency resource grid of T times and K frequency resources for each transmitter-receiver antenna pair as

$$\mathbf{H}_{t,n_r,n_t}^{(u)} = \text{DFT}_K \left(\left[\mathbf{H}_{t,n_r,n_t}^{(u)}[0], \dots, \mathbf{H}_{t,n_r,n_t}^{(u)}[L_p], \mathbf{0} \right] \right). \quad (6)$$

In total, the stacked channel tensor, $\mathbf{H} \in \mathbb{C}^{U \times T \times K \times N_r \times N_t}$, is the channel model for the MU-MIMO OFDM system. Precisely defining the time and frequency responses for every antenna pair is critical to accurately model the beam training process with specific resource elements allocated for pilots (reference signals) and data.

B. Reference signal receive power

We can now define the first metric of interest: the reference signal received power (RSRP). RSRP is one of the primary metrics that the receiver will measure during initial access for determining the channel quality. The base station will use this feedback to determine the strength of the signal, the initial code rate to be used, and what CSI-RS beamformers should be employed at the next iteration. We will assume the BS has three codebooks at any time: 1) SSB codebook $\mathbf{B}_{\text{SSB}} \in \mathbb{C}^{N_p \times L_{\max}}$, 2) CSI-RS codebook $\mathbf{B}_{\text{CSI-RS}} \in \mathbb{C}^{N_p \times N}$ where N is typically large and a small subset of beamformers is selected to be used based on the SSB feedback, and 3) feedback DFT codebook $\mathbf{B}_{\text{DFT}} \in \mathbb{C}^{N_p \times N_x O_H N_y O_V}$ with horizontal and vertical oversampling factors O_H and O_V . The number of logical ports, N_p , determines the digital precoding dimension and is equal to $N_x N_y$ in a fully digital array. The first two codebooks will be transparent to the UE and so the standards support an arbitrary output of a beam management algorithm. The feedback codebook must stay constant and is fully determined by the BS logical array size and oversampling factors, which are sent to the UE during initial access so that it can use the same codebook for feedback quantization.

RSRP is determined by measuring the received power during a given reference signal (SSB or CSI-RS). In the SSB case, the demodulation reference signal (DMRS), known at the transmitter and receiver, is used for RSRP measurement and decoding the master information block (MIB) provided in the SSB. The receiver operation for measuring the RSRP depends on the frequency range (FR) the system is operating at. In FR1 or sub-6GHz, the UE does not beamform (to avoid

additional beam training) during SSB reception and instead uses antenna selection or simply the first antenna for measurement. We will assume antenna selection for the $n_r \in \{0, \dots, N_r - 1\}$ antenna during SSB reception.

The SSB is transmitted over a band of K_{SSB} frequency resources at times $T_{i,\text{SSB}}$ for the i^{th} SSB using beamformer $\mathbf{f}_i \in \mathbf{B}_{\text{SSB}}$. While transmitting the reference signal, the rest of the band is still available for data transmission, so the total power is shared over all K resource blocks. In total, all L_{\max} SSBs are transmitted from the codebook \mathbf{B}_{SSB} . The large-scale channel SNR γ_u is separated from the small-scale fading to normalize channels while still accounting for users with stronger or weaker channel gains. Because the aggregated SNR value encompasses the relationship between the signal and noise strength (including both the thermal noise and the noise figure), the noise \mathbf{N} is modeled as IID, unit variance complex Gaussian random values. The RSRP is then

$$\text{RSRP}_i^{(u)} = \max_{n_r} \frac{1}{K} \sum_{k \in K_{i,\text{DMRS}}} \sum_{t \in T_{i,\text{DMRS}}} \frac{\gamma_u}{N_T} \left\| \mathbf{H}_{t,k,n_r}^{(u)} \mathbf{f}_i \right\|^2 + \left\| \mathbf{N}_{t,k,r} \right\|^2. \quad (7)$$

We will assume throughout the paper that all beamformers are normalized according to a per-symbol power constraint, i.e.

$$\left\| \mathbf{f}_i \right\|^2 = N_T. \quad (8)$$

Note that (7) is for a specific UE (u) and SSB (i), so the total SSB information aggregated at the base station is comprised of the RSRP and SSB index (SSBRI) for each of the UEs, denoted as (\mathbf{p}, \mathbf{m}) , and defined as

$$\mathbf{p} = \left\{ \max_i \text{RSRP}_i^{(u)} \right\}_{u=0}^{U-1} \quad (9)$$

$$\mathbf{m} = \left\{ \operatorname{argmax}_i \text{RSRP}_i^{(u)} \right\}_{u=0}^{U-1}. \quad (10)$$

It is worth noting that the actual SSBRI is not transmitted by the users, but rather, the time that the UE responds will correspond to a specific SSBRI. This is an efficient way to reduce the amount of bits used for feedback while still sharing the necessary information.

C. Channel state information reference signal

CSI-RS has many flexible configurations but we will use CSI type-II feedback (Release 16),

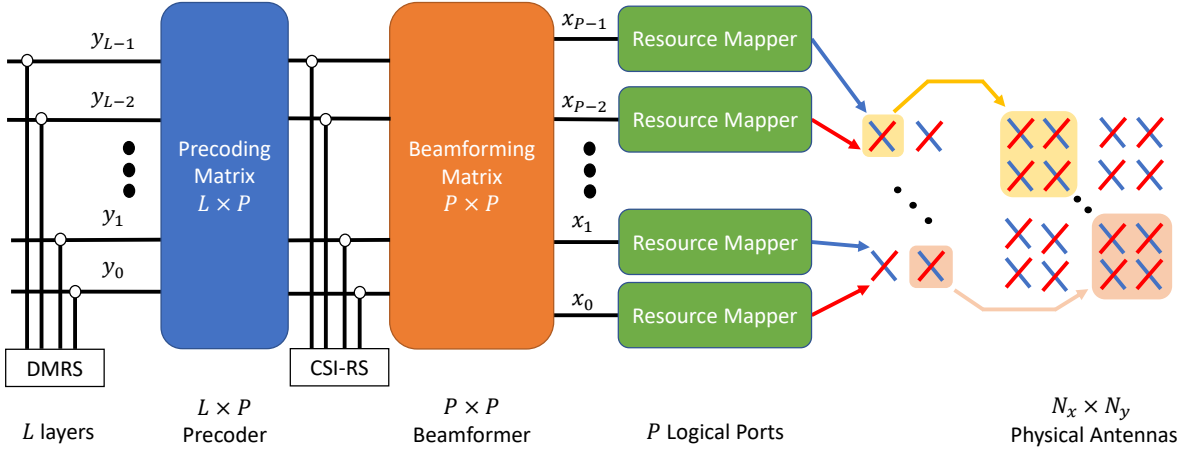


Fig. 2. The data processing flow from data streams (layers) to antenna outputs in 5G. First, the streams (and DMRS) are multiplexed according to the precoding matrix, which essentially assigns the layers to the ports. Then, the result, along with CSI-RS, is beamformed to the logical ports. The logical processes are then mapped onto OFDM resource grids and potentially beamformed again onto the corresponding physical antennas.

as our feedback baseline, which is intended for MU-MIMO with up to 2 layers per user [25]. For the next part of this section we will focus on the channel estimation and quantization for a single user (u) with CSI-RS beamformers $\mathbf{F}_{\text{CSI-RS}}$ selected from a set of possible beamformers $\mathbf{B}_{\text{CSI-RS}}$. The beam reception and selection process is identical to the RSRP and SSB selection in the previous subsection, so we do not re-mention it here.

Once a BS receives the SSB feedback for a new user, it can attempt to gather more precise CSI through channel state information reference signals. The CSI-RS are used for refined channel estimation, although the estimation is performed on the beamformed channel, rather than the physical channel. This enables larger hybrid arrays and improves the SNR for more accurate estimation. Readers are encouraged to review [3], [4], [7] for more details of the CSI feedback setup. The BS can use the SSB feedback to determine and transmit a set of CSI-RS signals with beamformers that are intended to further increase the RSRP compared to the SSB.

The choice of codebooks for CSI-RS has been studied to some degree, although the idea of using DFT beams is the most common setting [9], [12], [19], [26] and references therein. There is still some confusion in the literature about the various codebooks used in 5G NR. Often, it is assumed that the set of beamformers is selected from the same codebook as the codebook used for feedback, which is specified as an oversampled DFT codebook. There is no specification or need for the SSB or CSI-RS codebooks to be DFT codebooks, although using DFT beamformers

during CSI-RS has many advantages related to fast and efficient processing. For example, the CSI-RS selection can be done as a proportional DFT decomposition of the SSB beamformers. We will assume the CSI-RS codebook is comprised of oversampled DFT vectors throughout this paper, although additional investigations into a joint SSB-CSI-RS codebook algorithm are planned in future work. The selection of the CSI-RS beams from SSB decomposition is further refined in Section IV.

The CSI-RS process involves transmitting a set of pilots \mathbf{s} on the N_P ports along with P_{CSI} directive beamformers $\mathbf{F}_{\text{CSI-RS}} \subseteq \mathbf{B}_{\text{CSI-RS}}$ to ensure the UE can accurately estimate the effective channel. Each CSI-RS assignment will have at least P_{CSI} OFDM resource elements allocated for channel estimation in one resource block and it is assumed only one CSI-RS beam is active for a given resource to allow for a similar, interference-free beam selection as the SSB process. This is done by setting all other CSI-RS resources to be zero-power CSI-RS except the active one for the specified resources. In a dual-polarized system, the two polarizations are transmitted at the same time to enable co-polarization estimation. The whole CSI-RS process is allocated over NRB resource blocks, which is a configurable parameter to utilize wider bandwidths and noise averaging during channel estimation. For more information on the CSI-RS beam and port allocation please see [19] and references therein. The instantaneous SNR at the receiver with digital combining is

$$\text{SNR} = \max_{c \in P_{\text{CSI}}} \frac{1}{K_{\text{CSI}}} \sum_{k \in K_{c,\text{CSI}}} \sum_{t \in T_{c,\text{CSI}}} \frac{\gamma_u}{N_T} \frac{\left\| \mathbf{H}_{t,k}^{(u)} \mathbf{F}_{\text{CSI-RS}}[:, c] \right\|^2}{\left\| \mathbf{N}_{t,k} \right\|^2}. \quad (11)$$

Using the SNR according to (11), we can now focus on the effects of the directive beamformers $\mathbf{F}_{\text{CSI-RS}}$ on the channel estimation and overall performance.

Channel estimation accuracy depends on the number of pilot symbols and the received SNR of the pilots. The algorithm for UE channel estimation is not defined in the specification and is not explicitly critical for our system-level analysis. Instead, we highlight the effect that the SNR has on the accuracy of the channel estimation, which in turn affects the feedback choice and network performance during data transmission. For simplicity, we will assume channel estimation is done via a simple least squares algorithm so that only knowledge of the pilots is required. The resulting

mean squared error (MSE) of the channel estimate is related to the SNR by [24, section 3.7]

$$\text{MSE} = \frac{1}{\frac{N_{\text{pilots}}}{N_T} \text{SNR}}. \quad (12)$$

This trend is still the case for other estimation techniques such as minimum mean squared error (MMSE) with uncorrelated entries at relatively high SNR. In the case of correlations, (12) would act as a worst-case bound on the estimation performance. Thus, we can see that a primary feature of the beam management process is to enable more accurate channel estimation by beamforming the reference pilot signals. It might seem that the overhead of using multiple beams is wasted given that the number of pilots could alternatively be increased according to (12). The issue with such logic is that: 1) it assumes that the signal is always detectable over the noise floor, which is not necessarily the case for non-beamformed signals and 2) the beamforming can provide a gain on the order of 20dB or more, yet that would require 100 times more pilot symbols, far larger than the number of beams used. The estimated effective channel, $\widehat{\mathbf{H}}\mathbf{F}$, corresponds to the $N_R \times N_P$ coefficients after precoding. We will model the MSE as independent complex Gaussian random variables ($\mathcal{CN}(\mu, \sigma^2 \mathbf{I})$) such that

$$\widehat{\mathbf{H}}\mathbf{F} = \mathbf{H}\mathbf{F}_{\text{CSI-RS}} + \frac{1}{\sqrt{\frac{N_{\text{pilots}}}{N_T} \text{SNR}}} \mathcal{CN}(\mathbf{0}, \mathbf{I}). \quad (13)$$

The estimated effective channel is the first step in determining the feedback PMI.

There are multiple forms of PMI that could be given to the base station. For example, the user could provide PMI according to its desired beamformers (calculated via singular value decomposition). The base station could then use this information to beamform to a given user and null steer [27] the beams for other users. This puts the majority of the computational burden on the UE though and mathematically describing the process is unnecessary for our investigation. Instead, we follow models similar to [28] where the user provides PMI based on the effective channel estimate, rather than a set of precoders. This way the BS handles most of the computation, channel reconstruction, and precoder determination. The UE quantizes the channel estimate according to the feedback codebook for a specified L_{CSI} beams per rank up to the rank indicator R . The selection process is defined in [25, Section 5.2.2.2] for type-II codebooks. Assuming the feedback codebook is an oversampled DFT codebook with indices starting from the upper-leftward direction (relative to the cell panel) and continuing columnwise, we can make

use of efficient algorithms for channel decomposition. We present one such method in Algorithm 1, with an additional step of determining the orthogonal subset of beams provided in Algorithm 2. Although not presented here, type-I codebooks can also be used for SU-MIMO feedback and we use this form of feedback when comparing against the SU-MIMO results in Section V.

Algorithm 1 CSI Quantization

```

1: Given  $\widehat{\mathbf{HF}}$ ,  $\mathbf{B}_{\text{DFT}}$ ,  $L_{\text{CSI}}$ ,  $R$ 
2: for  $n_r \in \{1, 2, \dots, R\}$  do
3:    $\mathbf{c} \leftarrow \widehat{\mathbf{HF}}[n_r]\mathbf{B}_{\text{DFT}} \in \mathbb{C}^{N_x O_H N_y O_V}$ 
4:    $\mathbf{Q}_{n_r,0} \leftarrow \text{argmax } \mathbf{c}$ 
5:    $\mathbf{B}_{\text{ortho}} \leftarrow \{\mathbf{B}_{:,i} \in \mathbf{B}_{\text{DFT}} : \mathbf{B}_{\mathbf{Q}_{n_r,0}} \mathbf{B}_{:,i}^* = 0\}$  (see Algorithm 2)
6:    $\mathbf{c} \leftarrow \widehat{\mathbf{HF}}[n_r]\mathbf{B}_{\text{ortho}} \in \mathbb{C}^{N_x N_y - 1}$ 
7:   for  $\ell \in \{1, 2, \dots, L_{\text{CSI}} - 1\}$  do
8:      $\mathbf{Q}_{n_r,\ell} \leftarrow \text{argmax } |\mathbf{c}|$ 
9:      $\mathbf{C}_{\mathbf{Q}}[n_r, \ell] \leftarrow \mathbf{c}[\mathbf{Q}_{n_r,\ell}]$ 
10:     $\mathbf{c} \leftarrow \mathbf{c} \setminus \mathbf{c}[\mathbf{Q}_{n_r,\ell}]$ 
11:  end for
12: end for
13: return  $\mathbf{Q}, \mathbf{C}_{\mathbf{Q}}$  (The set of feedback indices and complex coefficients)

```

Algorithm 2 Orthogonal subset selection

```

1: Given  $\mathbf{Q}_{n_r,0}$ ,  $\mathbf{B}_{\text{DFT}}$  and DFT codebook settings  $N_X, O_X, N_Y, O_Y$ 
2:  $O_{X,0} \leftarrow \text{mod}(\lfloor \frac{N_{n_r,0}}{N_y O_Y} \rfloor, O_X)$ 
3:  $O_{Y,0} \leftarrow \text{mod}(\text{mod}(\mathbf{Q}_{n_r,0}, N_Y O_Y), O_Y)$ 
4:  $\mathbf{B}_{\text{ortho}} \leftarrow \{\}$ 
5: for  $n_x \in \{1, 2, \dots, N_X\}$  do
6:   for  $n_y \in \{1, 2, \dots, N_Y\}$  do
7:      $i = n_x(N_Y O_Y O_X) + O_{X,0}(N_Y O_Y) + n_y(O_Y) + O_{Y,0}$ 
8:      $\mathbf{B}_{\text{ortho}} \leftarrow \{\mathbf{B}_{\text{ortho}}, \mathbf{B}_{\text{DFT}}[:, i]\}$ 
9:   end for
10: end for
11:  $\mathbf{B}_{\text{ortho}} \leftarrow \mathbf{B}_{\text{ortho}} \setminus \mathbf{B}_{\text{DFT}}[:, \mathbf{Q}_{n_r,0}]$ 
12: return  $\mathbf{B}_{\text{ortho}}$  (The orthogonal DFT subset)

```

The CSI report will contain the CSI-RS indicator (CRI), the rank of the channel estimate, the RSRP, and the PMI feedback beams \mathbf{Q} , as well as 4 bit amplitude and 8-PSK phase values, $\mathbf{C}_{\mathbf{Q}}$, for the corresponding complex values for each $[n_r, \ell]$ feedback beam from \mathbf{c} in Algorithm 1. In

this paper, we will ignore the amplitude and phase quantization to focus on the effects of the codebooks, SNR, and feedback. It is also notable that the CSI report can contain both wideband and narrowband components for a degree of frequency selective precoding. The number of narrowband components is small, at most $BWP = 8$ in FR1, to mitigate the growing feedback and complexity. All of the previous and subsequent steps are defined for $BWP = 1$, but extending to frequency selective feedback and precoding is straightforward. We investigate how the amount of feedback (L_{CSI} , BWP) impacts performance in Section V.

D. Precoders

After the CSI-RS period, the base station must determine the precoder that serves a group of users, often with the goal of maximizing the sum rate or proportional fair rate. Until this stage, all of the downlink transmissions have been multi-cast in the sense that the same data is intended for all users. Therefore, there is no interference assuming a well-designed OFDM cyclic prefix and subcarrier spacing is used with accurate synchronization. In contrast, the downlink data transmission carries different data for each user, resulting in interference between data streams. The remainder of this section outlines the channel reconstruction process, precoder selection, and achievable spectral efficiency in the downlink channel.

First, the BS can reconstruct the channel estimate with the corresponding complex scaling factor \mathbf{C}_Q as

$$\widehat{\mathbf{HF}}[n_r] = \sum_{i=0}^{L_{CSI}-1} \mathbf{C}_Q[n_r, i] \mathbf{B}_{DFT}[:, \mathbf{Q}_{nr,i}] \quad \forall n_r. \quad (14)$$

Then, assuming the training sequence was well-chosen such that \mathbf{F}_{CRI} is right-invertible (i.e. at least one training symbol is used for each port and the training sequence is generated according to 5G pseudo-random sequences), the channel reconstruction can be performed successfully. We will re-introduce the UE (u) notation here to allow for aggregating all user channels in subsequent steps by

$$\widehat{\mathbf{H}}_u = \widehat{\mathbf{HF}}_{CSI-RS}^\dagger. \quad (15)$$

In the case of DFT beams, this process simply becomes an IDFT operation [19], which is significantly more efficient than the matrix inverse of an $N_P \times N_P$ matrix. The efficiency at this step is critical to quickly utilizing the feedback and is one reason we will tailor our algorithm

to integrate with a DFT codebook for CSI-RS. Aggregating the results for each user, we obtain the downlink channel estimate $\widehat{\mathbf{H}} \in \mathbb{C}^{U \times N_R \times N_P}$

$$\widehat{\mathbf{H}} = \{\widehat{\mathbf{H}}_u\}_{u=1}^U. \quad (16)$$

The base station can design the precoders for the set of estimated channels using any form of precoding, although, zero-forcing (ZF) and regularized ZF (RZF) are commonly used as a linear precoding algorithm. Herein we will assume a regularized zero forcing precoder is used with regularization determined to minimize the signal-to-leakage noise ratio [24, section 9.9]. The RZF is built up for each user as

$$\mathbf{F}_u = \sqrt{N_T} \frac{(\sum_{i=0}^{U-1} \gamma_i \widehat{\mathbf{H}}_i^* \widehat{\mathbf{H}}_i + U N_T \mathbf{I})^{-1} \widehat{\mathbf{H}}_u^*}{\left\| (\sum_{i=0}^{U-1} \gamma_i \widehat{\mathbf{H}}_i^* \widehat{\mathbf{H}}_i + U N_T \mathbf{I})^{-1} \widehat{\mathbf{H}}_u^* \right\|}. \quad (17)$$

The UE will also perform a combining strategy based on the previously determined rank. In this work we will assume an LMMSE receiver is used to maximize the signal-to-interference noise ratio (SINR) for any precoder, using the embedded DMRS to determine the combined channel and precoder. The resulting SINR at resource element (t, k) for a given user u and layer r with equal power allocation per user is obtained as

$$\text{SINR}_{t,k,u,r} = \frac{1}{K} \frac{\mathbf{F}_u^*[:, r] \tilde{\mathbf{H}}_{u,t,k}^* \left(\sum_{i=0}^{U-1} \tilde{\mathbf{H}}_{u,t,k} \mathbf{F}_i \mathbf{F}_i^* \tilde{\mathbf{H}}_{u,t,k}^* + \frac{U N_T}{\gamma_u} \right)^{-1} \tilde{\mathbf{H}}_{u,t,k} \mathbf{F}_u[:, r]}{1 - \mathbf{F}_u^*[:, r] \tilde{\mathbf{H}}_{u,t,k}^* \left(\sum_{i=0}^{U-1} \tilde{\mathbf{H}}_{u,t,k} \mathbf{F}_i \mathbf{F}_i^* \tilde{\mathbf{H}}_{u,t,k}^* + \frac{U N_T}{\gamma_u} \right)^{-1} \tilde{\mathbf{H}}_{u,t,k} \mathbf{F}_u[:, r]}. \quad (18)$$

While the SINR expression (18) appears complicated, it is a simplified ratio between the signal power for the data stream (u, r) versus the interference power of all other streams with normalization by the large-scale SNR γ_u .

Finally, the most critical metric in the wireless network is the sum SE or sum rate when applied to a specific bandwidth. A fairness constraint can also be applied, however, we have not specified any form of scheduling so we are most interested in maximizing the sum spectral efficiency or rate. Assuming Gaussian signaling, the achievable spectral efficiency, $\text{SE}_{u,t}$, is

$$\text{SE}_{u,t} = \sum_{k=1}^{K-1} \sum_r \log_2(1 + \text{SINR}_{t,k,u,r}). \quad (19)$$

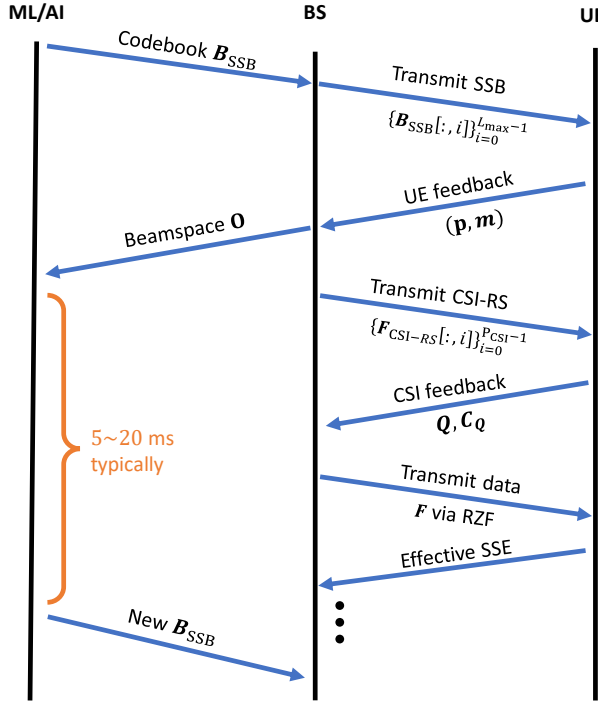


Fig. 3. A timing diagram of the process for codebook learning and evaluation. The AI/ML engine provides new codebooks at each SSB interval for the base station (BS). At each CSI-RS period, the BS transmits pilots using the CSI-RS codebook, which is determined based on the SSB codebook and feedback. The CSI-RS feedback is used to determine the precoder used for data transmission.

In the final post-processing, we consider the effective sum SE, which accounts for the overhead due to beam training by removing the corresponding time/frequency resources due to training and feedback of the beam management system (T_{BM}, K_{BM}) from the spectral efficiency calculation

$$\text{Eff-SSE} = \frac{1}{K} \sum_{t \notin T_{BM}} \sum_{k \notin K_{BM}} \sum_{u \in U} \sum_r \log_2(1 + \text{SINR}_{t,k,u,r}). \quad (20)$$

With this goal and the beam management framework in mind, we can now define the problem statement and contributions of this work.

IV. BEAMSPACE-CODEX

In this section, we present the Beamspace-Codex which is a neural network architecture and processing setup that is used to generate the SSB codebooks. We start by introducing the beamspace observation that provides a consistent basis for a learning algorithm using dynamic codebooks. We then present the supervised learning formulation that enables convergent and dynamic codebooks. Finally, we define the neural network architecture that enables learning the

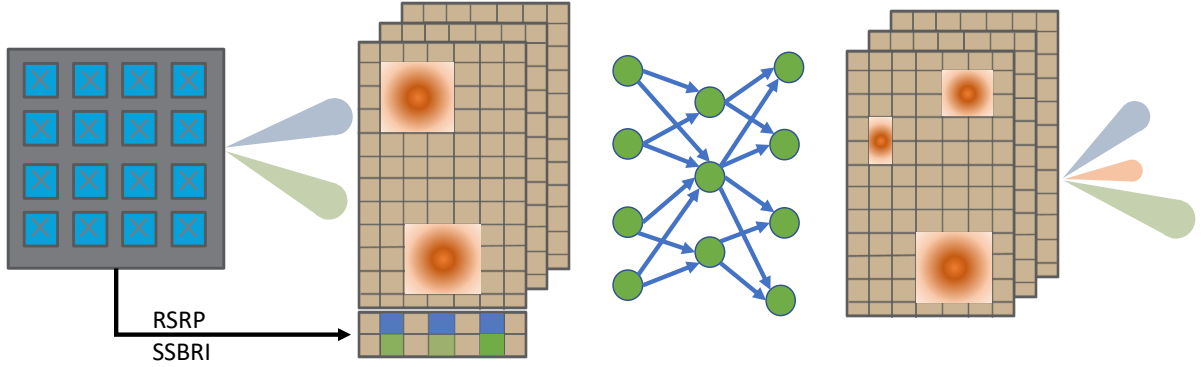


Fig. 4. A depiction of the BSC processing. The feedback is converted to an angular representation and the strongest directions are identified based on the feedback reported. This unifies the various codebooks with a consistent input dimensionality even with varying numbers of users or even antenna sizes.

underlying relationship between the beamspace observation and the SSB codebook. The full methodology—processing, architecture, training, and evaluation—is critical to integrating wireless domain knowledge and physical structure into the learning algorithm.

One of the primary steps in designing an appropriate neural network is formulating the input-output relationship to be conducive and consistent for learning. There are two problems with neural networks within the context of 5G beam management. First, the SSBRI feedback corresponds to a beamformer from a codebook that was used previously, which does not provide a consistent representation or meaning with dynamic codebooks. Second, the number of users is not constant within a cell, so the size of the feedback and data dimension changes over time. Although there are specific ways to overcome dynamic data sizes, it often requires sacrificing hardware optimizations and impedes inference and training times.

We propose transforming the codebook into the beamspace domain. The beamspace [29] is an angular representation of a beamformer corresponding to the array factor evaluated over a range of directions. This ensures that regardless of the specific codeword, or even physical antenna dimension, the corresponding input from a set of previous beamformers still represents a two-dimensional grid of projections. The beamspace conversion for N_{x0} azimuth directions and N_{y0}

elevation direction is calculated as

$$\boldsymbol{\theta}_{N_m} = \frac{1}{\pi}[0, 1, \dots, N_m - 1] \quad (21)$$

$$\mathbf{U}_{N_s, N_m} \triangleq [\mathbf{a}_{N_s}(\boldsymbol{\theta}_0), \dots, \mathbf{a}_{N_s}(\boldsymbol{\theta}_{N_m-1})] \in \mathbb{C}^{N_s \times N_m} \quad (22)$$

$$\mathbf{F}_{\text{SSB}}^{(N_x N_y)}[i] = [\mathbf{F}_{\text{SSB}}[i, 0 : N_x]^T, \mathbf{F}_{\text{SSB}}[i, N_x : 2N_x]^T, \dots, \mathbf{F}_{\text{SSB}}[i, 0 : N_y N_x]^T] \quad (23)$$

$$\mathbf{O}[i] = \mathbf{U}_{N_{x0}, N_x} \mathbf{F}_{\text{SSB}}^{(N_x N_y)}[i] \mathbf{U}_{N_{y0}, N_y} \forall i \in L_{\max}. \quad (24)$$

The codebook must first be converted from a vector of size N_T to the planar dimensions $N_X \times N_Y$ in (23) before the beamspace conversion in (24). In addition to the angular representation, the input is also concatenated with the feedback corresponding to the number of users reporting each beam and the sum RSRP after min-max normalization. Note that the beamspace conversion is a reversible operation, so we also train the network to predict the beamspace of the desired output, rather than direct beamforming coefficients. The predicted beamformers are obtained in post-processing, and the computational complexity can be controlled by changing the observation sizes N_{x0} and N_{y0} . With the pre/post-processing defined, we can now define the supervised learning environment and desired outputs used for training.

Supervised learning provides many advantages over unsupervised or reinforcement learning paradigms when there is a desired solution. While some problems do not have optimal or ideal solutions, the task of determining beamforming vectors that maximize the power to a set of users does have an optimal solution if CSI is available. To that end, we assume a dataset of channels has been built up or simulated to allow for offline training, although our site-specific results in Section V suggest that transferring a learned model between sites is still more effective than DFT codebooks. Then, the solution to maximize the power received for a user is the right singular vectors (RSV) of the singular value decomposition of the channel [2], also often known as eigen-beamforming. In the MU-MIMO OFDM case, this means taking the RSVs corresponding to the L_{\max} strongest singular values of all users over the 240 subcarriers used by the SSB process. Additionally, the timing of the beams is important because the fast fading experienced by the channel causes variations of up to about 1/2 dB over the time span of one set of SSBs. To build a true supervised setting, however, we must sacrifice the time relationships of the data. In particular, we do use information from past SSB feedback beyond the previous step. This limitation is noticeable but allows for significantly improved convergence compared

to a reinforcement learning setting. The process is limited to a two-step relationship where we include the previous codebook and feedback to help design the next codebook. We now have a supervised framework and pre/post-processing step that converts the previous codebook and RSV codebook to the beamspace domain. The final component of the Beamspace-Codex is the neural architecture that facilitates efficient learning.

At the root of the formulation is a question of translation—from the initial beamspace to the RSV beamspace with only the number of users and reported RSRP aid the translation. Inherently, it is not obvious how the limited feedback information could be used to recover the optimal codebook, however, there is some underlying information available by the selection of one beam over $L_{\max} - 1$ other options. Additionally, the environment and user densities follow a pattern that is also possible to exploit. We considered many different network architectures including convolutional neural networks, autoencoders, and convolutional autoencoders, as well as modern architectures like vision transformers [30] and diffusion models [31]. Throughout our testing, the fully connected architecture showed the strongest results with an average of 1dB higher average RSRP than other architectures, while also being the most computationally efficient architecture. We propose a multi-layer network with significant regularization through dropout comprised of 6 densely connected layers with parameters and sizes determined through Bayesian hyperparameter tuning and defined in Table I. The model is trained using an Adam optimizer [32] with early stopping and cosine learning rate decay with restarts [33]. Training is performed with a 550,000 sample training dataset following the setup in Section VI with validation and test sets each from an unseen portion of the data corresponding to 160,000 and 80,000 samples respectively. Gradients are determined by the cosine distance between the RSV beamspace and the neural network-predicted beamspace. The choice of the loss function is critical for performance as the same network architectures trained on mean squared error results in significantly worse ($> 5\text{dB}$) performance due to focusing on the pixel-wise magnitude, rather than the relative magnitude or direction of the RSV beamspace.

V. SIMULATION SETUP

In order to accurately evaluate the performance of ML-designed codebooks, we require a highly accurate channel simulator coupled with a flexible framework that retains the timing of the 5G beam training process. It is also important to keep in mind the metric of interest, which is

TABLE I
BEAMSPACE-CODEX NETWORK PARAMETERS.

Layer	Primary Parameter	Activation Func.	Output Dimension
Flatten			$(2L_{\max}(N_{x0} + 2)(N_{y0} + 2))$
Fully Conn.	144 Neurons	ReLU	(144)
Dropout	0.2 Rate		(144)
Fully Conn.	1808 Neurons	ReLU	(1808)
Dropout	0.4 Rate		(1808)
Fully Conn.	272 Neurons	ReLU	(272)
Dropout	0.4 Rate		(272)
Fully Conn.	240 Neurons	ReLU	(240)
Fully Conn.	80 Neurons	ReLU	(80)
Fully Conn.	$(2N_{x0}N_{y0}L_{\max})$ Neurons	ReLU	$(N_{x0}, N_{y0}, 2L_{\max})$
Reshape			$(N_{x0}, N_{y0}, 2L_{\max})$

primarily sum spectral efficiency. Although RSRP is also a valuable metric, if a high RSRP reported from the SSB does not also translate to a high SNR during CSI-RS, then the overall system performance is not improved. We, therefore, integrate channel generation from QuaDRiGa [34] with a post-processing suite that enables an initial access scenario, beamspace generation, codebook determination, and evaluation of the network performance after accounting for beam management overhead.

QuaDRiGa generates channels through a stochastic process with additional features for spatial consistency, correlations, and spherical wave modeling. In our simulations, we simulate 200 users scattered over a base station sector site. The BS is equipped with an $N_x = 4$, $N_y = 8$ planar array using a 3GPP 3D antenna model with half-wavelength spacing. Each user has $N_r = 4$ similar antennas all tuned for a 3.5GHz carrier frequency. 10% of users are given a vehicular mobility pattern such that they travel along a roadway through the center of the cell with speeds normally distributed with mean 25m/s and variance 5m/s. The remaining users are uniformly scattered within 450m and travel in any direction with speeds uniformly drawn from an interval of [0, 3]m/s. Channel distributions follow a 3GPP urban macrocell environment [35] and channels are sampled over a bandwidth of 100MHz every 1ms for 2s. Large user numbers (200) are necessary at this step to build up a database that is spatially and environmentally consistent. In the final section of the results, we address how the model generalizes to a new setting with different environmental

parameters and different roadway locations. Once the channels are generated, post-processing is necessary to produce a realistic setting and build up the algorithm's datasets. The process starts by randomly selecting a number of active users (uniformly between [2, 12]) and gathering the channels and time slots from the channel set. Then randomly selecting L_{\max} DFT beams for the 'prior' codebook and calculating the RSV codebook. The codebooks are converted to beamspace representations and stored in a dataset along with the SSB feedback from a subset of the active users where each active user is assigned an 80% probability of its feedback being included. This represents a true initial access channel where not all users are previously known and introduces an additional regularization term into our algorithm to prevent over-focusing on known users. It is assumed that UEs utilize antenna selection for the RSRP reception during the SSB process, digital combining for CSI-RS, and LMMSE combining during data transmission as defined in the system model.

VI. SIMULATION RESULTS

It is critical to extensively evaluate a neural network model to fairly represent and compare it against traditional methods. In our previous work [36], we have considered a learning threshold as a minimal metric for determining if meaningful relationships have been learned by the network. In realistic wireless channels, such settings are much harder to characterize, so we instead benchmark the performance against industry-standard DFT techniques and RSV codebooks assuming CSI were known perfectly. This helps to identify the upper-performance limits (with respect to maximum RSRP) as well as the minimal performance needed to justify moving beyond traditional codebooks. We then use our robust simulation framework to better understand how the various codebooks and type-II CSI feedback parameters affect network performance in realistic FR1 channels. In the first subsection, we look at the RSRP performance of the SSB process with various codebooks. Then we look at the subsequent SNR achieved during CSI-RS, where the CSI-RS beams are determined by decomposing the SSB beam into a subset of DFT beams with an equal proportion to the number of users selecting the beam during SSB. For example, if there are 4 users that each select a different SSBRI, then the P_{CSI} CSI-RS beams would be evenly divided between the 4 corresponding SSB beams. For arbitrary codebooks, the CSI-RS beams are selected by decomposing the initial codebook in the same way as Algorithm 1 and selecting the strongest beam components from \mathbf{C}_Q . In the next subsection, we provide an in-depth evaluation of the CSI-RS process without BSC codebooks. In that section we evaluate

performance based on the effective downlink SE after overhead due to beam training, uplink feedback, and an additional signaling overhead factor of 10%. Uplink feedback is assumed to be the only resource usage and we assume a worst-case scenario where users transmit with MCS0 from Table 5.1.3.1-1 [25] and users are allocated at the resource block level to account for additional allocation overhead. User selection during the data phase is performed based only on the knowledge at the BS by first estimating the sum spectral efficiency achieved with the imperfect CSI for all users with $\{1, 2\}$ data layers. The best estimated SE combination is selected and used, although such a format is naturally suboptimal, even with perfect CSI, due to a lack of rank adaption. User selection is not the focus of this investigation, so we only use an exhaustive search over the reconstructed channel knowledge to provide a basic but reasonable scheduling algorithm. We also look at the SE with rank-1 non-PMI beamforming where RZF is not employed, the channel is not estimated, and the only feedback is obtained from the SSB phase, with user selection and precoder determination simply being the SSB codeword with the strongest reported user RSRP. This is often an envisioned beam management strategy for sparse mmWave channels with short, low-latency feedback, but is not assumed to be effective in sub-6GHz channels due to the rich scattering environment.

A. RSRP and SNR

The RSRP is a basic metric that can be used to directly demonstrate the ability of the neural network to output a valuable SSB codebook. Following the SSB process, we also highlight the performance that the dynamic codebook provides when selecting CSI-RS beams as a decomposition of the SSB codebook. While these two metrics—RSRP and SNR—do not ultimately characterize the network performance as a result of the codebook algorithm, they do provide meaningful insight into the performance of various codebook methods. Figure 5a shows the empirical cumulative distribution function (CDF) of the RSRP reported using various codebook/beamforming methods. Without any beamforming, more than 50% of users would be below the minimum RSRP for signal detection, which is often around -120dBm . The SSB codebooks are decomposed into CSI-RS codebooks in Figure 5b, where we see the RSV codebook is *not* consistently the best SSB codebook when directly decomposed into CSI-RS codebooks. We can understand this as a result of the rich scattering environment that causes the RSV to not effectively decompose into a small number of incoherent DFT components. While RSV beamformers maximize the

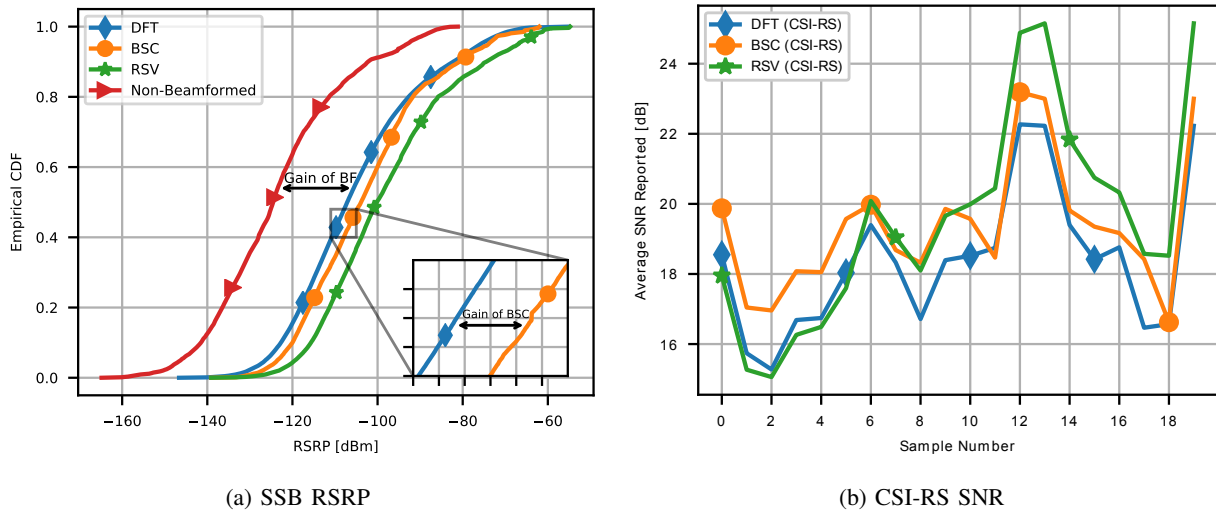


Fig. 5. Two plots of the codebook performance measuring (a) RSRP received during SSB and (b) SNR during CSI-RS reception. During the SSB stage, each of the codebooks is used directly and then in (b) the SSB codebooks are decomposed to form the CSI-RS codebook. Non-beamformed transmission presents a significant loss in performance while the learned BSC codebook shows gains of about 3dB over traditional DFT beams. While RSV beamforming is RSRP-maximizing during the SSB, the DFT decomposition of an RSV codebook is not necessarily SNR-maximizing due to multipath propagation.

received power for a user, this maximization is based on the signal coherently combining and is not well-represented by a narrow DFT beam.

B. Feedback

In this subsection, we highlight the critical aspect of feedback in 5G CSI type II and four quantities affecting the feedback. The size of the CSI-RS codebook is related to the channel estimation SNR because larger CSI-RS codebooks, made of orthogonal DFT beamformers, will result in equivalent or higher SNR compared to smaller codebooks with the same channels and feedback. We use the feedback from a DFT SSB codebook to characterize the performance of larger or smaller CSI-RS codebooks in Figure 6a. Although the estimation performance before quantization will always improve with a larger codebook, there is also a modest amount of overhead with larger P_{CSI} so that there is little spectral efficiency gain beyond $P_{\text{CSI}} \geq 8$.

In the next comparison, the feedback quantization is evaluated by modifying the parameter L_{CSI} in type-II formats. We can see from Fig. 6b that higher resolution feedback is beneficial, with effective data rate gains of almost 3 times when the resolution is improved from $L_{\text{CSI}} = 1$ to $L_{\text{CSI}} = 32$. From there on, the other parameters CSI-RS resource block allocation (NRB) and the number of frequency selective resources (BWP), are less influential compared to the quantization

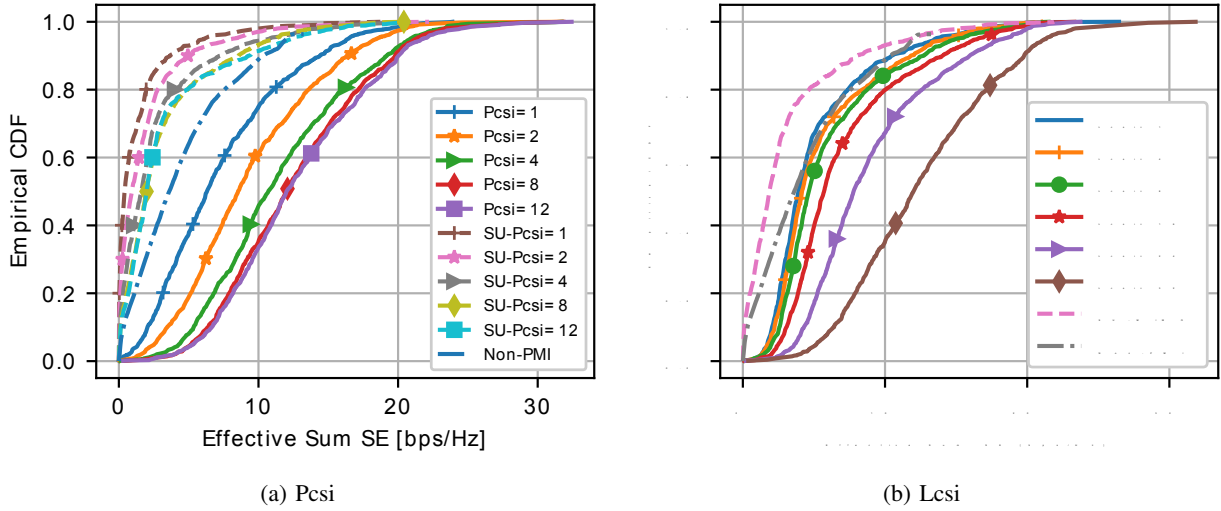


Fig. 6. Evaluation of the effects of active CSI-RS codebook size (a) and quantization using L_{CSI} multipath feedback components. We can use the size of the codebook as a means of looking at how codebook optimization improves performance because the overhead with larger P_{CSI} is very small compared to the overhead of type-II feedback. SU-MIMO results using type-I PMI are shown by dashed lines while MU-MIMO results are shown by solid lines and Non-PMI refers to rank 1 beamforming using the CRI. SU-MIMO does not include multipath feedback so only a single SU-MIMO result is shown in (b). Other parameters are set to $L_{CSI} = 32$ for (a), $P_{CSI} = 16$ for (b), BWP = 1, NRB = 24. We can see that the loss from using $L_{CSI} = 4$ (Release 16 maximum) compared to $L_{CSI} = 32$ is more detrimental than restricting the system to a single CSI-RS beamformer.

resolution. Most of the modest performance gains achieved with multiple frequency selective precoders and larger downlink CSI-RS resource usage are offset by the increasing overhead resulting in negligible or even destructive performance impacts. Joining the information from Figures 6a-7a, a good balance of feedback and performance can be achieved with a setting of $L_{CSI} = 32$, BWP = 1, NRB = 24, $P_{CSI} = 8$. It is important to note that the current 5G Release 16, even with enhanced type-II feedback, only supports $L_{CSI} \leq 6$, which means most situations will only yield about 1.5 times higher effective spectral efficiency relative to SU-MIMO, and essentially equivalent performance to the non-PMI beamforming. Perhaps even more surprising is that using a single CSI-RS beam ($P_{CSI} = 1$) has less degradation than using $L_{CSI} = 8$ feedback beams per rank, relative to the best performance. This suggests that feedback limitations are more likely to restrict MU-MIMO performance in sub-6GHz systems compared to codebook optimization or accurate channel estimation.

C. Site generalization

Up to now, we have used a test set of data drawn from the same statistical environment as the training set. While a network operator will likely gather data for a specific site, here we

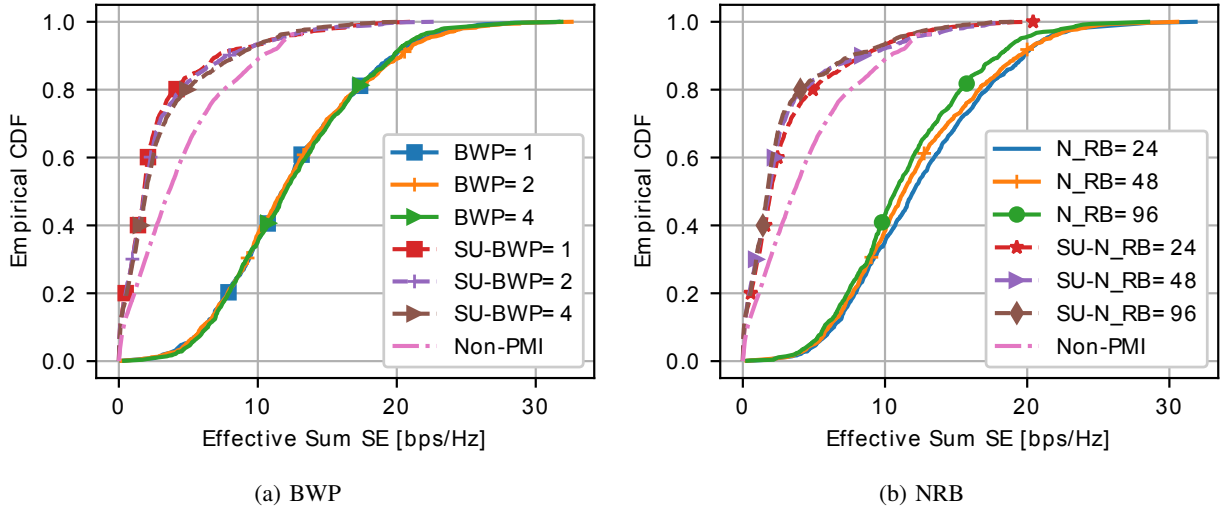


Fig. 7. A comparison of the effective spectral efficiency with different numbers of frequency selective precoders BWP and varying the number of resource blocks (NRB) per BWP. It is assumed that $L_{\text{CSI}} = 32$, $P_{\text{CSI}} = 16$, $\text{NRB} = 24 \times \text{BWP}$ in (a) and $\text{BWP} = 1$ in (b). While increasing the number of resource blocks, therefore increasing the number of pilots, increases the channel estimation performance, the increased overhead causes the performance to decrease in (b). In comparison, the size of BWP increases the overhead linearly, yet the performance is essentially equivalent. Therefore we see that frequency selective feedback and beamforming is not necessarily advantageous when overhead is accounted for.

examine the impact of testing on a new distribution of data. We simulate a new environment with completely different user distributions and mobility patterns. Now 50% of users are vehicular with roadways defined in new locations and a new stochastic realization of the channel environment. In Figure 8 the agnostic (orange) data is obtained without updating the model, whereas the fine-tuned data (blue) shows the results after we allow for 60s of retraining on data from the new environment. Our time limit is arbitrary and could ultimately be orders of magnitude shorter than the timescale a network operator might use to update the model, but corresponds to approximately 1% of the training time used in our setup for a balance of fine-tuning and generalization. It can be seen in Figure 8 the performance in the new environment (agnostic) is significantly worse relative to the RSV. The performance loss is noticeably improved during fine-tuning, especially for the lowest 10% of users.

VII. CONCLUSION

In this paper, we presented a novel framework for learning dynamic codebooks for sub-6GHz 5G NR. We first set up a system with multiple UEs each equipped with a uniform linear array to receive from a base station with an excess of antennas in a fully digital planar array. We simulate realistic sub-6GHz channels using QuaDRiGa and build a post-processing framework

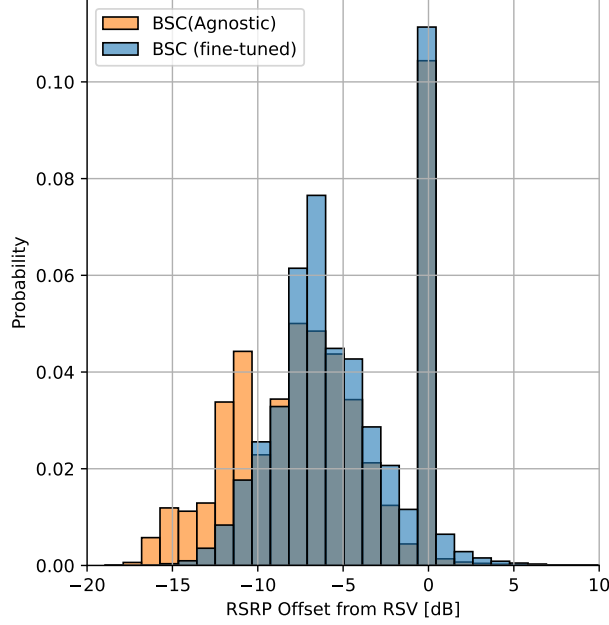


Fig. 8. Histogram representing the performance delta between BSC and RSV codebooks in the agnostic setting and after fine-tuning. It can be seen that the worst-case differences are resolved and in some cases (when more users are present than SSB beams) the RSV codebook can be outperformed.

for evaluating the system performance of SSB and CSI-RS codebooks and feedback. We used this framework to address two questions related to codebook performance in 5G: 1) Can machine learning design more effective initial access codebooks? 2) How should feedback be configured for MU-MIMO in sub-6GHz environments?

We first proposed a codebook transformation based on beamspace projections that allows for efficiently and consistently representing codebooks in a format conducive to learning. This beamspace representation allows for circumventing challenges with dynamic user numbers, changing codebooks, and even deploying across different physical antenna array sizes. Using the beamspace as a convenient translation tool, we designed a neural architecture, Beamspace-Codex, based on a densely connected structure to translate SSB feedback into a new codebook. The proposed method directly integrates with current 5G standards and improves SSB RSRP by 3 – 5dB on average, while also efficiently updating to fit new environments and distributions with only 1% of the original compute used during training.

Second, we focused on feedback in 5G type-II formats, which are highly configurable yet under-researched due to the complexity and dependency on the SSB, CSI-RS, and feedback codebooks.

We propose a simple and efficient algorithm for decomposing the channel estimate into a set of oversampled DFT beams to be used for feedback according to 5G specifications. The beam management framework is then used with BSC dynamic codebooks to quantify the resolution and frequency-selectivity of feedback needed to overcome the additional overhead of type-II feedback in MU-MIMO operations. We find that the channel quantization resolution, determined by the number of feedback DFT beams, is a limiting factor in the performance of MU-MIMO in current standards. In future work, we will extend the investigation to multi-sector scenarios with implicit and explicit coordination to further optimize the beam management process.

REFERENCES

- [1] R. M. Dreifuerst and R. W. Heath, "Massive MIMO in 5G: How beamforming, codebooks, and feedback enable larger arrays," *in submission to IEEE Commun. Mag.*, 2023.
- [2] V. Raghavan *et al.*, "Beamforming Tradeoffs for Initial UE Discovery in Millimeter-Wave MIMO Systems," *IEEE J. Sel. Top. Signal Process.*, vol. 10, no. 3, pp. 543–559, Apr. 2016.
- [3] Y. Heng *et al.*, "Six key challenges for beam management in 5.5G and 6G systems," *IEEE Commun. Mag.*, vol. 59, no. 7, pp. 74–79, Jul. 2021.
- [4] M. Giordani *et al.*, "A tutorial on beam management for 3GPP NR at mmwave frequencies," *IEEE Commun. Surv. Tutorials*, vol. 21, no. 1, pp. 173–196, Jan. 2019.
- [5] A. Alkhateeb, O. El Ayach, G. Leus, and R. W. Heath, "Channel estimation and hybrid precoding for millimeter wave cellular systems," *IEEE J. Sel. Top. Signal Process.*, vol. 8, no. 5, pp. 831–846, Oct. 2014.
- [6] E. Becirovic, E. Bjornson, and E. G. Larsson, "Combining reciprocity and CSI feedback in MIMO systems," *IEEE Trans. Wirel. Commun.*, May 2022.
- [7] Samsung, "Massive MIMO for new radio," Dec. 2020. [Online]. Available: <https://www.samsung.com/global/business/networks/insights/white-papers/1208-massive-mimo-for-new-radio/>
- [8] B. Li *et al.*, "On the efficient beam-forming training for 60GHz wireless personal area networks," *IEEE Trans. Wireless Commun.*, vol. 12, no. 2, pp. 504–515, 2013.
- [9] V. Va *et al.*, "Inverse multipath fingerprinting for millimeter wave V2I beam alignment," *IEEE Trans. Veh. Technol.*, vol. 67, no. 5, pp. 4042–4058, May 2018.
- [10] Y. Wang, N. J. Myers, N. González-Prelcic, and R. W. Heath, "Deep Learning-based Compressive Beam Alignment in mmWave Vehicular Systems," *arXiv*, pp. 1–33, 2021. [Online]. Available: <https://arxiv.org/abs/2103.00125>
- [11] Y. Wang, N. J. Myers, N. González-Prelcic, and R. W. Heath, "Site-specific online compressive beam codebook learning in mmWave vehicular communication," *IEEE Trans. Wirel. Commun.*, pp. 1–14, 2021.
- [12] Q. Xue *et al.*, "Beam management in ultra-dense mmWave network via federated reinforcement learning: An intelligent and secure approach," *IEEE Trans. Cogn. Commun. Netw.*, 2022.

- [13] J. Yang, W. Zhu, and M. Tao, “Deep learning for hierarchical beam alignment in mmWave communication systems,” in *Proc. of the IEEE Global Communications Conference*, 2022.
- [14] Z. Xiao, T. He, P. Xia, and X.-G. Xia, “Hierarchical codebook design for beamforming training in millimeter-wave communication,” *IEEE Trans. Wireless Commun.*, vol. 15, no. 5, pp. 3380–3392, 2016.
- [15] R. Shafin *et al.*, “Self-tuning sectorization: Deep reinforcement learning meets broadcast beam optimization,” *IEEE Trans. Wirel. Commun.*, vol. 19, no. 6, pp. 4038–4053, Jun. 2020.
- [16] W. Xia *et al.*, “A deep learning framework for optimization of MISO downlink beamforming,” *IEEE Trans. Commun.*, vol. 68, no. 3, pp. 1866–1880, Mar. 2020.
- [17] Y. Heng, J. Mo, and J. G. Andrews, “Learning site-specific probing beams for fast mmwave beam alignment,” *IEEE Trans. Wirel. Commun.*, vol. 21, no. 8, pp. 5785–5800, 2022.
- [18] R. M. Dreifuerst, R. W. Heath, and A. Yazdan, “Massive MIMO beam management in sub-6 GHz 5G NR,” in *Proc. of the IEEE Veh. Technol. Conf.*, 2022, pp. 1–5.
- [19] G. Morozov, A. Davydov, and V. Sergeev, “Enhanced CSI feedback for FD-MIMO with beamformed CSI-RS in LTE-A Pro systems,” in *Proc. of the IEEE Veh. Technol. Conf.*, Jul. 2016, pp. 1–5.
- [20] C. K. Wen, W. T. Shih, and S. Jin, “Deep learning for massive MIMO CSI feedback,” *IEEE Wirel. Commun. Lett.*, vol. 7, no. 5, pp. 748–751, 2018.
- [21] J. Kim, H. Lee, and S.-H. Park, “Learning robust beamforming for MISO downlink systems,” *IEEE Communications Letters*, vol. 25, no. 6, pp. 1916–1920, 2021.
- [22] M. Chen *et al.*, “Deep Learning-based Implicit CSI Feedback in Massive MIMO,” *IEEE Trans. Commun.*, vol. 70, pp. 935–950, Dec. 2022.
- [23] 3GPP, “TS 38.213 V16.7.1 NR; Physical layer procedures for control.”
- [24] R. W. Heath Jr. and A. Lozano, *Foundations of MIMO Communication*. Cambridge University Press, 2018.
- [25] 3GPP, “TS 38.214 V16.7.1 NR; Physical layer procedures for data.”
- [26] A. Singh and S. Joshi, “A survey on hybrid beamforming in mmWave massive MIMO system,” *J. Sci. Res.*, vol. 65, no. 01, pp. 201–213, 2021.
- [27] L. Godara, “Application of antenna arrays to mobile communications. ii. beam-forming and direction-of-arrival considerations,” *Proceedings of the IEEE*, vol. 85, no. 8, pp. 1195–1245, 1997.
- [28] M. R. Castellanos *et al.*, “Channel-Reconstruction-Based Hybrid Precoding for Millimeter-Wave Multi-User MIMO Systems,” *IEEE J. Sel. Areas Commun.*, vol. 12, no. 2, pp. 383–398, May 2018.
- [29] A. Sayeed, “Deconstructing multiantenna fading channels,” *IEEE Transactions on Signal Processing*, vol. 50, no. 10, pp. 2563–2579, 2002.
- [30] Z. Liu *et al.*, “Swin transformer: Hierarchical vision transformer using shifted windows,” in *Proc. of the IEEE Int. Conf. Comput. Vis.*, Mar. 2021, pp. 9992–10 002.
- [31] J. Ho, A. Jain, and P. Abbeel, “Denoising diffusion probabilistic models,” 2020. [Online]. Available: <https://arxiv.org/abs/2006.11239>

- [32] D. Kingma and J. Ba, “Adam: A method for stochastic optimization,” *International Conference on Learning Representations*, Dec. 2014.
- [33] I. Loshchilov and F. Hutter, “SGDR: Stochastic gradient descent with warm restarts,” 2016. [Online]. Available: <https://arxiv.org/abs/1608.03983>
- [34] S. Jaeckel, L. Raschkowski, K. Börner, and L. Thiele, “QuaDRiGa: A 3-D multi-cell channel model with time evolution for enabling virtual field trials,” *IEEE Trans. Antennas Propag.*, pp. 3242–3256, 2014.
- [35] B. Mondal *et al.*, “3D channel model in 3GPP,” *IEEE Commun. Mag.*, vol. 53, no. 3, p. 16–23, Mar. 2015.
- [36] R. M. Dreifuerst and R. W. Heath, “SignalNet: A low resolution sinusoid decomposition and estimation network,” *IEEE Trans. Signal Process.*, vol. 70, pp. 4454–4467, Aug. 2022.